

3-D modeling of the generation and propagation of acoustic T-waves at seafloor spreading ridges

Jean Lecoulant^a, Claude Guennou^a, Laurent Guillon^b, Jean-Yves Royer^a

^a Université de Brest & CNRS, Lab. Géosciences Océan, Plouzané, France

^b Ecole Navale, IRENAV, Brest, France

Contact author:

J. Lecoulant, Institut Universitaire Européen de la Mer, Laboratoire Géosciences Océan (UMR6538), Place Nicolas Copernic, F-29280 Plouzané, France

Phone : +33(0)2 98 49 88 94

E-mail : jean.lecoulant@univ-brest.fr

Abstract: *Seafloor spreading ridges are generally isolated in the middle of the oceans and remote from seismometers deployed on land. As a result, their low-level seismic activity and near-field phenomena related to earthquakes are poorly known. Deploying hydrophones to record hydroacoustic waves generated by undersea earthquakes, known as T-waves, is an alternative way to monitor this low-level seismic activity. The rapid attenuation of seismic waves in the Earth crust is overcome by the excellent acoustic properties of the ocean. To better understand the interaction of a seismic event with the seafloor and the resulting generation of the T-wave acoustic phase, we use a 3D spectral finite-element code – SPEC-FEM3D – that jointly models the propagation of seismic waves in a solid medium (the Earth crust) and of the acoustic waves in the fluid medium (the ocean). Using simplified configurations, we investigate the dependency of T-wave generation on the topography of the sea-bottom. The time-function used to model the earthquake source is adapted to near-field modeling. The seafloor topography, hence the size and shape of the conversion zone, determines the presence of T-waves and the amplitude, shape and duration of the signal. Our first results confirm the generation of T-waves, even when the source is offset relative to a seamount or a trough on the seafloor, but in all cases their modal propagation is slower than the sound-speed. Our results thus highlight the importance of 3D-effects in the generation and propagation of T-waves, which must be taken into account to fully describe and understand T-waves recorded by hydrophones.*

Keywords: *T-waves, underwater acoustics, spectral element model, seismo-acoustic conversion, 3D-effects*

1. Introduction

The submarine seismic and volcanic activity occurring at seafloor spreading ridges generates a great amount of low-frequency acoustic waves. The seismic waves generated by an earthquake propagate in the Earth crust till they reach the sea-bottom. Depending on the local topography, they may convert to acoustic waves propagating into the water column [e.g. 1]. These waves are known as T-waves (tertiary waves), because they may convert back onshore into seismic waves and arrive at seismographs after the P- and S-waves. T-waves receive wide attention, since their study can improve our understanding of seafloor spreading ridges [e.g. 2].

Seismic data acquired on land by seismographs generally provide no or little information on the low-level seismic activity of mid-ocean ridges, due to the rapid attenuation of seismic waves in the Earth crust. On the contrary, T-waves recorded by hydrophones take advantage of the excellent acoustic properties of the ocean, such as the very long-distance propagation with little attenuation when propagating in the SOFAR (SOund Fixing And Ranging) channel.

To better understand the T-waves generation on the seafloor and their propagation, we use a 3D spectral finite-element code (SPECFEM3D) that jointly models the propagation of seismic waves in a solid medium (the Earth crust) and of acoustic waves in the fluid medium (the ocean) [3, 4]. Using simplified configurations, we test the effect of the seafloor topography on the generation of T-waves. The first section presents the model parameters and the second section presents the simulations and discusses the results.

2. Model parameters

The calculation domain for the simulations is a parallelepiped, 100x100 km wide and 20 km thick. It is horizontally divided in a 3 km thick fluid medium (the ocean) underlain by a 17 km thick solid medium (the Earth crust). All sides, except the top (sea) surface, are absorbing layers to avoid unwanted reflection that would pollute the results. The medium densities are constant and set at 1100 kg.m⁻³ for the water layer and 3200 kg.m⁻³ for the Earth crust. The sound velocity in the water is also set constant (1500 m.s⁻¹), as the speed of P-waves (5000 m.s⁻¹) and S-waves (3000 m.s⁻¹) in the crust. There is no attenuation either in the solid medium or in the fluid one.

Three simplified topographies are used to test the generation of T-waves: a seamount, a ridge and a trough. The idealized seamount is built by rotating about the z-axis a Gaussian curve with a 15 km base and 2000 m height. The linear ridge is built by translating the same Gaussian cross-section along the x-axis. The trough is simply a reversed Gaussian seamount. These simple topographies, with an appropriate mesh, allow a relatively short calculation time (typically half an hour with 84 parallel processors).

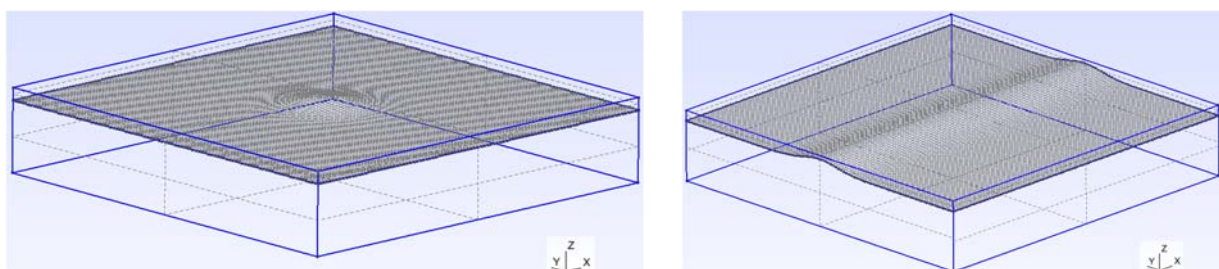


Fig. 1: Calculation domain with the meshed surface for a Gaussian seamount (left) and a linear Gaussian ridge (right). The box size is 100 x 100 km. The solid and fluid media are 17 km and 3 km thick, resp.

The source is located 7 km under the seafloor, at the center of the domain, and is simulated by a 0.5 s half-duration Heaviside function. A Heaviside signal is less usual than a Gaussian signal, but it is more realistic for near-field modeling. In any case, the elastic behavior of the solid medium turns the Heaviside waveform into a Gaussian signal before it reaches the crust/ocean interface. The focal mechanism is an isotropic explosion, which ensures that the T-waves pattern will only reflect the effect of topography and not the radiation pattern of the source. The chosen seismic moment ($M_0 = 3.98 \cdot 10^{23}$ N.m) corresponds to a medium magnitude earthquake ($M_w = 5.0$).

Finite element modeling allows to extract the waveform in any mesh cell. To monitor the generated waves, we distributed “hydrophones” in the water column, in two different ways: every 50 m along a radius from the center of the model, at a constant depth of 1500 m, and every kilometer over a grid covering the whole domain, at a constant depth of 500 m. The line will provide a high-resolution view of the different wave-phases, the grid will provide an overview of the full pressure field radiating from the epicenter. Note that the line of sensors intersects the seamount or the ridge, whose top are only 1000 m below the sea-surface.

3. Results and discussion

Waves produced by the earthquake can clearly be identified in a Hovmöller diagram (Fig 1, left). In this distance-time diagram, the slope of the arrivals gives the speed of the waves. The first arrivals are P-waves propagating at the speed chosen for the model (5 km s^{-1}); they are followed the Scholte waves at their theoretical speed (90% of S-waves speed). After 7 s, the most energetic waves form a group propagating at a slower speed (1227 km s^{-1}) than the sound speed. A 2D-Fourier transform of the Hovmöller diagram turns it into a frequency-wave number diagram (Fig 1, right). This diagram clearly shows that the simulated waves follow the dispersion curves of the nine first acoustic modes in the case of an isovelocity perfect waveguide. It thus demonstrates that in this configuration, the earthquake generates acoustic waves, or T-waves, travelling in the water column by modal propagation.

Inversion of actual T-waves from a network of hydrophones generally assume that they propagate at the full sound speed [e.g. 2]. Our results suggest that this assumption is not correct since, here, T-waves travel at a mean velocity 18% slower than the sound-speed.

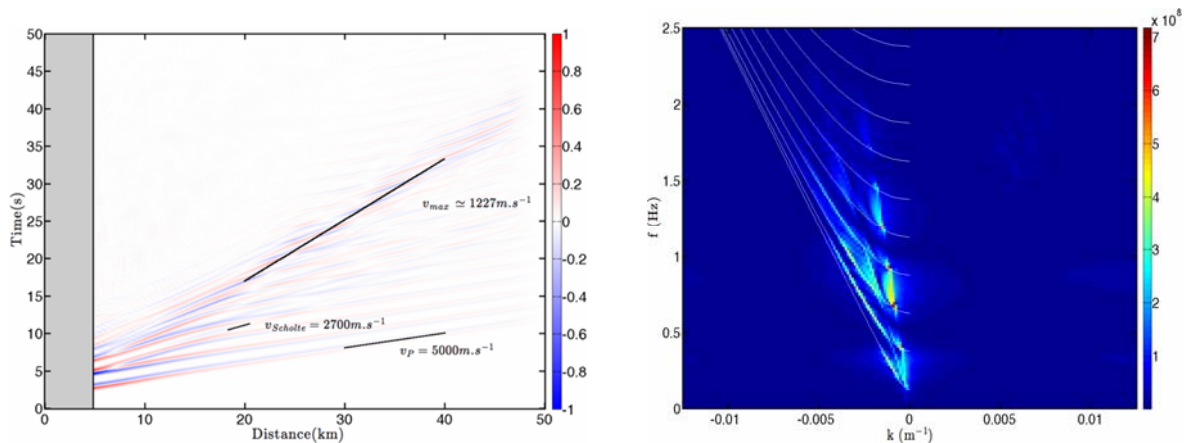


Fig. 2: (Left) Hovmöller diagram of normalized pressure in the case of an isotropic explosion under a Gaussian seamount. The grey area shows the seamount width at the depth of the sensors (1500 m below sea-level). (Right) Frequency-wave number diagram in the case of an isotropic explosion under a Gaussian mount. The theoretical dispersion curves of the ten first acoustic modes in a perfect isovelocity waveguide are shown in white.

The results from the model with a linear ridge highlights additional 3D-effects. Figure 3 (left) compares the time-signal at a hydrophone (i.e. mesh cell) 500 m below sea-level, 45 km away from the center of the seamount or ridge (i.e. epicenter) and perpendicularly to the ridge. Both signals show the same arrival-times. However, the amplitudes of the peak T-wave arrivals, 30 s after the beginning of the run, are about twice larger for the ridge case. This can be explained by a larger size of the seismic/acoustic conversion zone in the case of the mountain range. Yet, the number of generated acoustic modes remains the same, as shown by the frequency-wave number diagram in the ridge case (Fig. 3, right).

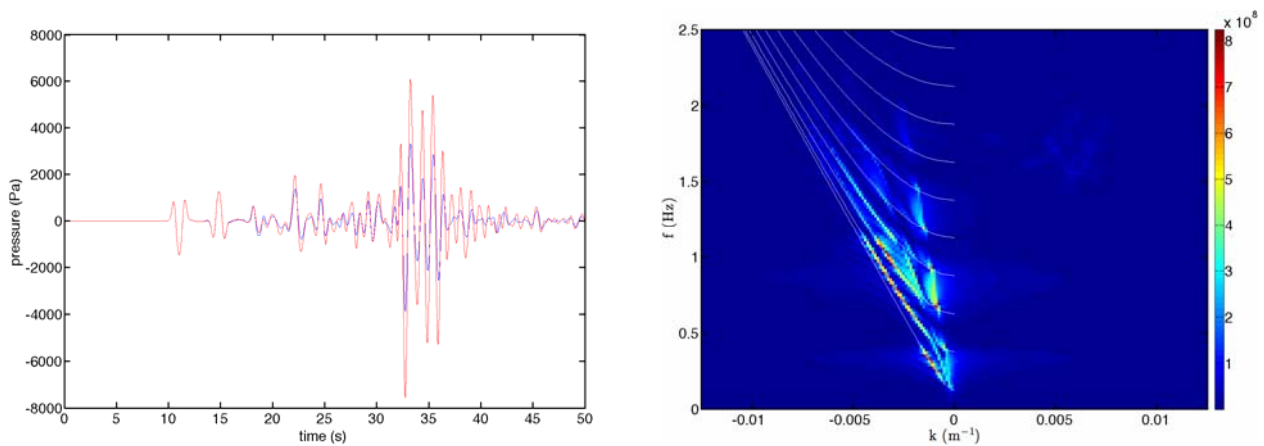


Fig. 3: (Left) Comparison between time-signals measured by a hydrophone 45 km away from the epicenter in the case of a Gaussian seamount (blue) and of a Gaussian mountain range (red). (Right) Frequency-wave number diagram in the case of an isotropic explosion under a Gaussian mountain range (to be compared with Fig. 2 left).

To test whether T-wave conversions can occur away from an epicenter, which remains a matter of debate [5], we offset the source 25 km from the axis of the seamount (Fig. 4 left). T-waves begin to be radiated after the P-waves reach the mount, firstly from the slope nearest to the source. As the P-waves progress, T-waves are radiated from all sides of the seamount. With a source 25 km away from the axis of a Gaussian trough (Fig. 4 right), T-waves are radiated by the slope farthest to the source. The T-waves are mainly emitted in a direction away from the source.

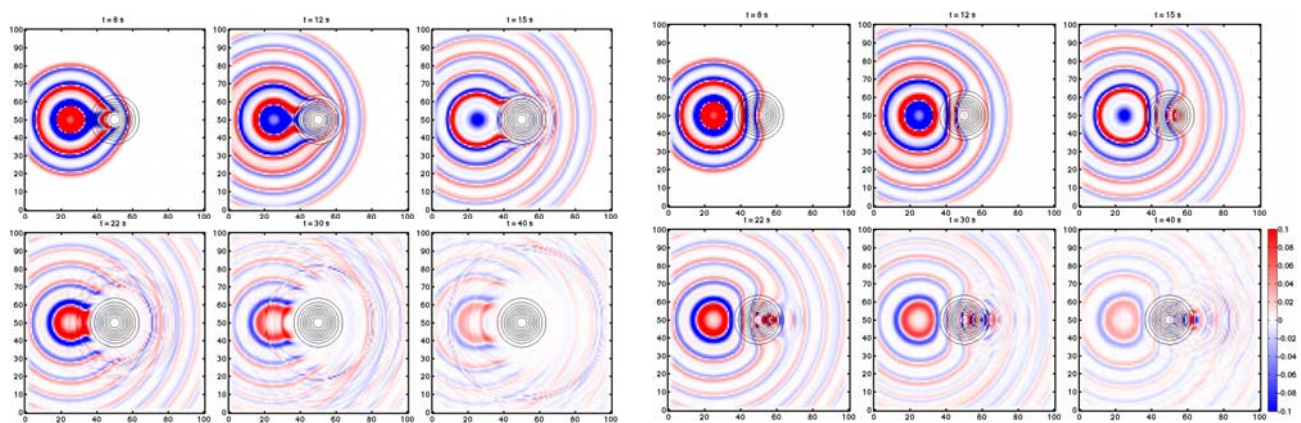


Fig. 4: Plane view of the normalized pressure field at a 1500m depth, for an explosive source offset relative to a Gaussian seamount (left) and trough (right). Isobaths every 250 m are shown in black. Note that the top of the seamount intersects the sensor plane. Snapshots at 8, 12, 15, 22, 30 and 40 s after the explosion.

4. Conclusion

Addressing the question of T-wave generation at the seafloor in 3 dimensions does show some 3D effects of the topography, even in simplified configurations. In this respect, the spectral finite element code SPEC3D [3, 4] proves to be a very effective tool. Our simple simulations show that T-waves propagate as acoustic modes and, surprisingly, at a velocity slower than the sound-speed. The energy of T-waves increases with the size of the conversion zone (i.e. size of the slopes). T-waves are also generated when the source is offset relative to the topography. Seamount, ridge and trough generate different T-wave radiation patterns. Future work will focus on the effect of the rugosity of the seafloor to test the idea of wave-scattering [6, 7], and, beyond that, will test more realistic models with a layered oceanic crust, a Munk velocity profile in the water-column, and more realistic sources (e.g. normal or strike-slip fault focal mechanisms).

5. Acknowledgments

J. Lecoulant is supported by a joint PhD grant from the *Délégation Générale de l'Armement* (DGA) and the University of Brest (UBO). The SPEC3D code was run on Datarmor, a massive computing facility common to several research institutions at the westernmost tip of Brittany (France).

6. Bibliography

- [1] **Okal, E. A.**, The generation of T waves by earthquakes, *Adv. Geophys.*, 49: 1-65, 2008.
- [2] **Fox, C. G., Matsumoto, H. and Andy Lau, T.-K.**, Monitoring Pacific Ocean seismicity from an autonomous hydrophone array, *J. Geophys. Res.*, 106 (B3): 4183-4206, 2001, doi: 10.1029/2000JB900404.
- [3] **Komatitsch, D. and J. Tromp**, Introduction to the spectral element method for 3D seismic wave propagation, *Geophys. J. Int.*, 139 (3): 806-822, 1999.
- [4] **Tromp, J., Komatitsch, D., and Liu, Q.**, Spectral-element and adjoint methods in seismology, *Commun. Comput. Phys.*, 3 (1): 1-32, 2008.
- [5] **Chapman, N. R. and Marett, R.**, The directionality of acoustic T-phase signals from small magnitude submarine earthquakes, *J. Acoust. Soc. Am.*, 119 (6): 3669-3675, 2006, doi: 10.1121/1.2195073.
- [6] **De Groot-Hedlin, C. D. and Orcutt J. A.**, Excitation of T-phases by seafloor scattering, *J. Acoust. Soc. Am.*, 109 (5): 1944-1954, 2001, doi: 10.1121/1.1361057.
- [7] **Park, M., Odom, R. I. and Soukup, D. J.**, Modal scattering: A key to understanding oceanic T waves, *Geophys. Res. Lett.*, 28: 3401-3404, 2001.

